Tensile properties of Ag-EVOH electrospinning nanofiber mats for large muscle scaffolds

Chuanwei Zhang[1], Dandan Liu[1], Chao Xu[1]*, Dianzi Liu[1,3], Bin Wang[1,2]

[1]*School of Mechanical Engineering, Xi'an University of Science and Technology, No.58 Yanta Rd, Xi'an, Shaanxi, P.R. China, 710054*

[2] *School of Engineering and Design, Brunel University, UK*

[3] *School of Engineering and Mathematics, University of East Anglia, UK*

Abstract

Large muscle defect negatively influences people's life, the common treatment is muscle transplantation but limited by donor source, large area wound etc. Therefore, a muscle tissue scaffold with superimposed vascular network was developed. For ensuring the performance of fascia layer which alternated by Poly(ethylene-co-vinyl alcohol) (EVOH) nanofiber mats encapsulated with Ag, the mechanical properties and water vapour transmission of different samples (7.5%, 10%, 12.5% EVOH solution densities with 0.02g/ml, 0.05g/ml, 0.08g/ml of Ag respectively) were mainly discussed. Meanwhile, the main parameters (voltage, tip-to-collector distance, solution density, concentration of Ag) were compared to find their influence on fabricating nanofibers.

Key words: large muscle defect, electrospinning, nanofiber, experimental parameters, tensile properties, Young's moduli, strain rate, water vapour transmission

1.0 Introduction

Large muscle defect is a serious problem which harms thousands of lives every year. Although significant achievements have been made by the researchers in the field, such as muscle transplantation, which is an effective way to repair large muscle defect. However, the

application of muscle transplantation is limited due to the limitation of available muscle resources, large area skin wound, allograft donor source and immune rejection, etc [1-2]. The loss of skeletal muscle tissue and function may be solved in the future with the development of tissue engineering, especially the progress in muscle tissue regeneration and functional reconstruction of skeletal muscle tissue engineering [3-5].

Researches confirm that the key of muscle tissue engineering is the oriented arrangement and differentiation of muscle cells [6]. There are two common methods for cell oriented arrangement. First one, the directional arrangement of cells on the surface of the scaffold is achieved through the constraint of the scaffold structure or surface chemical modification. The current methods of scaffold micro manufacturing are Soft Etching [7], Pressure Forging [8], Electrospinning [9-10], Photocopying and solvent casting Manufacturing Technology [11-12], etc. Second one is planting myoblast and satellite cells in scaffold [13-14], some stimulus (like the mechanical stimulation [15-16] or stimulation of Electricity and magnetism [17-19]) from outside are then applied to achieve the orientation of the cells on the scaffold and differentiate into the direction of the muscle tissue, so finally the repair of the scaffold in the tissue is completed.

In this study, a muscle tissue engineering scaffold with superimposed vascular network (Figure 1) was designed by simulating the muscle structure in vivo [20]. Scaffold 1 and 2 were prepared by stereolithography and mould turning technology, perfusion vascular network was fabricated in TG enzyme cross-linked hydrogel interior, meanwhile, EVOH nanofibers were fabricated by electrospinning to simulate fascia layer of muscle tissue, then finally obtained the muscle tissue engineering scaffold by positioning assembly. In order to

arrange and differentiate the cells on the scaffold, a dynamic culture platform was designed and built in vitro, as shown in Figure 2. The experimental platform of bio-reactor consists of three parts: stretching mechanism, irrigation system and power system. This platform supplies a mechanical tensile test system with a sealed chamber and controls the tensile strength of soft tissue exactly. Moreover, the perfusion of chamber and vascular network can be performed respectively to simulate the state of blood flow in vivo and study the speed and pressure of irrigation to provide the basis of researches for proliferation, prolongation and differentiation of cells.

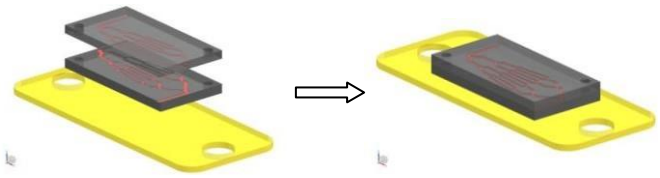

Fig. 1 Assembly process of muscle scaffold

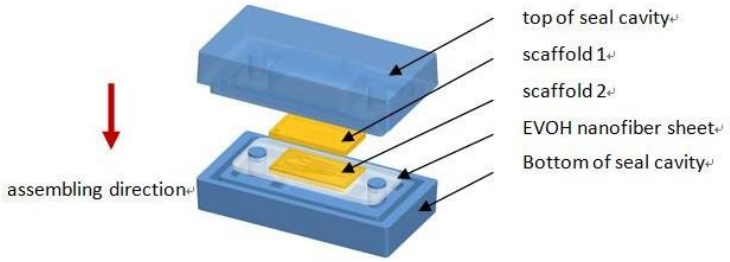

(a)

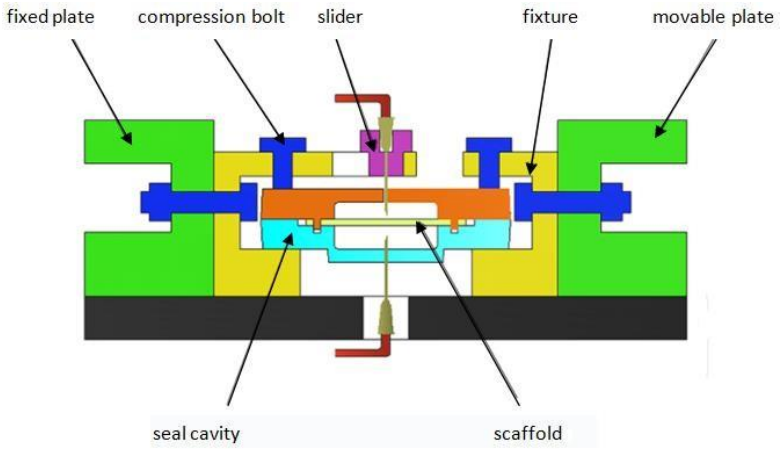

(b)

(c)

Fig. 2 Dynamic perfusion-stretching culture platform in vitro (a) Assembly process of scaffold and seal chamber (b) Schematic diagram of perfusion—stretching on scaffold (c) Dynamic perfusion - stretching culture platform

Fascia layer plays an important role in the dynamic culture. On one hand, hydrogel is fragile, electrospun mats could provide mechanical support during the mechanical stretching after the hydrogel was packaged by the mats. Poly (ethylene-co-vinyl alcohol) (EVOH) is the raw material which has been used in the previous and this study [21], the mechanical properties of pure EVOH nanofiber mats have been proved which satisfies the dynamic perfusion-stretching test [22]. On the other hand, there are a lot of components and

complicated structures of the dynamic culture platform, and the dynamic perfusion-stretching tests normally take over 10 days, therefore, the possibility of pollution during the tests is very high (over 50%) which influences the experimental results. To solve this problem, we aim to fabricate a self-antibacterial EVOH scaffold for preventing pollution by combining the electrospinning technique and silver nanoparticles during the long experimental process.

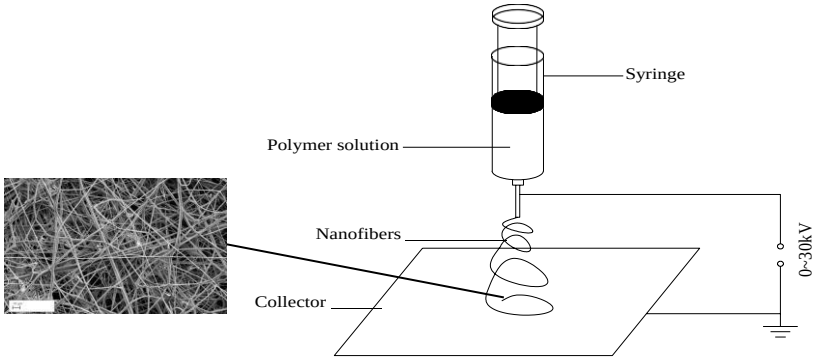

Fig. 3 Electrospinning system

Electrospinning is a well-known method which fabricates very fine nanofiber mats, it is already used in the wound dressing field [23-24]. The principle of the system (Figure 3) is that the charged droplet at the needle is gradually stretched with the electric field force to form “Taylor Cone” and ejected then. The nanofibers were fabricated in the process of ejection and overlapped on collector to obtain the EVOH nanofiber mats. The properties of the mats obtained with different raw materials are diverse [25]. The objective of this study is to fabricate better performance sheets which include the mechanical properties, antibacterial abilities and perviousness to simulate fascia layer.

In our previous studies, poly (ethylene-co-vinyl alcohol) (EVOH) nanofibers with 10% of solution density have already been used in the experiments. The results of the experiment proved the tensile stress of EVOH nanofiber mats achieve the standard as analogue of the

fascia layer. Therefore, silver (Ag) with long time and effective antibacterial ability [26] were considered to add to the EVOH solution to fabricate self antibacterial nanofiber mats. Furthermore, the new EVOH nanofiber mats need to be retested for the confirmation of the influences on tensile strength and perviousness (water vapour transmission test) with different concentrations of Ag.

Thus, in this study, different concentrations of Ag nanoparticle (0.02g/ml, 0.05g/ml and 0.08g/ml) were used as antibacterial substance which encapsulated with nanofiber. Besides, to compare the effect of Ag on nanofibers comprehensively, different densities of EVOH solutions (7.5%, 10% and 12.5%) were placed on each concentration, therefore, 9 groups of samples can be obtained and their tensile strength were tested and compared to verify the influence of concentration on the mechanical properties. Moreover, the microstructures and diameters of the nanofibers have been taken and measured by the SEM. To satisfy the clinical requirements and emphasizing prominent, we have quantified the effectiveness between the fabrication parameters and the mechanical properties including the Young's moduli, Yield stresses and the effect of different strain rates. In addition, the water vapour transmission rate of Ag EVOH nanofiber mats were quantified to match the situation in vivo.

This paper is arranged in the following sections: first of all, the electrospinning fabrication technology and the material used are introduced. Secondly, the microstructures and nanofibers' diameters performed and measured by the Scanning Electron Microscope. Thirdly, the tensile tests on thin sheets with different concentrations of EVOH and Ag are quantified, followed by the water vapour transmission test and discussions of the results.

2.0 Experimental methods

2.1 Materials

In this study, Poly(ethylene-co-vinyl alcohol) (EVOH) (Fig 4a) was used to fabricate the nanofibers, it was bought from Sigma-Aldrich (Batch number: 12822PE) in granular form. The Ag particles that adhered to EVOH nanofibers of products were provided by $AgNO_3$ (Fig 4b) which was purchased from Huaxing Experiment Technology Co., Ltd. in Shaanxi.

In the preparation of the solution for the electrospinning, 10ml blending solvent which mixed by 7ml isopropanol and 3ml deionized water was poured into a conical flask with granular EVOH (0.75g, 1g and 12.5g). Then, putting them on a magnetic stirrer for full stirring with 70~80℃ in a water bath. After around 2~3h, added granular $AgNO_3$ respectively with different masses(0.2g, 0.5g, 0.8g) and still stirring till the solution be transparent(Fig 4c).

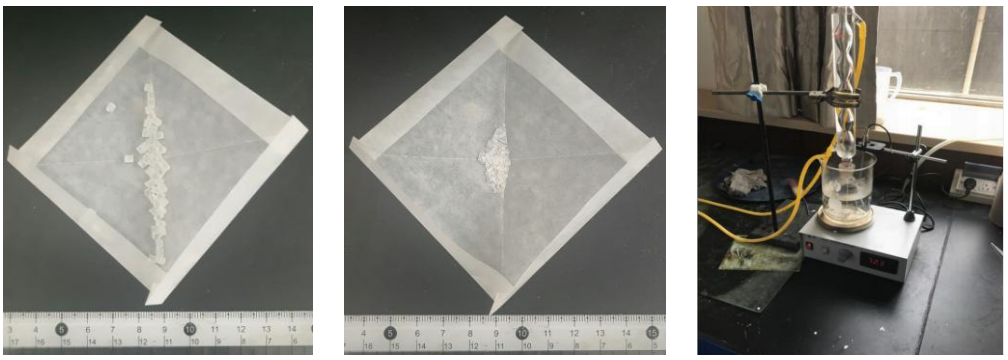

(a)EVOH (b)$AgNO_3$ (c)preparation for solution

Fig. 4 Preparation before electrospinning

2.2 Electrospinning process

The electrospinning system carries out various parameters, such as the voltage of 0~30kv, the distance between syringe and collector of 0~40cm, the ambient temperature of 0~100℃, the collector rotation speed of 0~140r/min, the pushing speed of syringe and the

height of collector etc.

In this study, the voltage used was 15-25kV, the distance between syringe and collector was 15-35cm. In order to reduce the blockage of needles by crystallization, the temperature was improved to 45℃approximately.

After fabricating the samples, the microstructure was observed by Scanning Electron Microscope (SEM). Figure 5 shows the general distribution of nanofibers mats. Meanwhile, the diameter of nanofibers was measured for comprehending the interrelations between the main parameters. Moreover, each fiber is attached with different size of granular substances. To verify the element of the particles, it was tested by EDX (shown in Figure 6) which provides the Ag existing proof in nanofibers from Figure 6a and 6b, they are the diagram and table of spectrum.

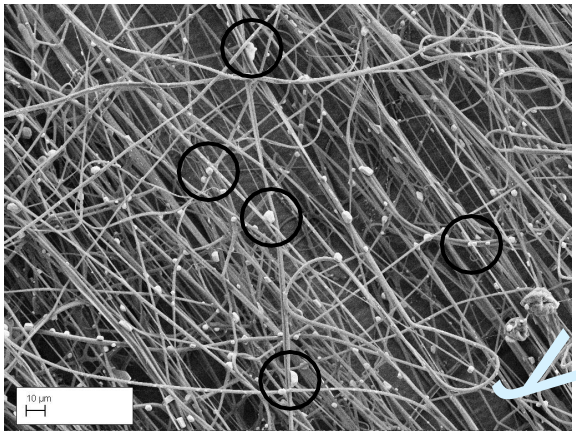

Fig. 5 general distribution of nanofibers mats

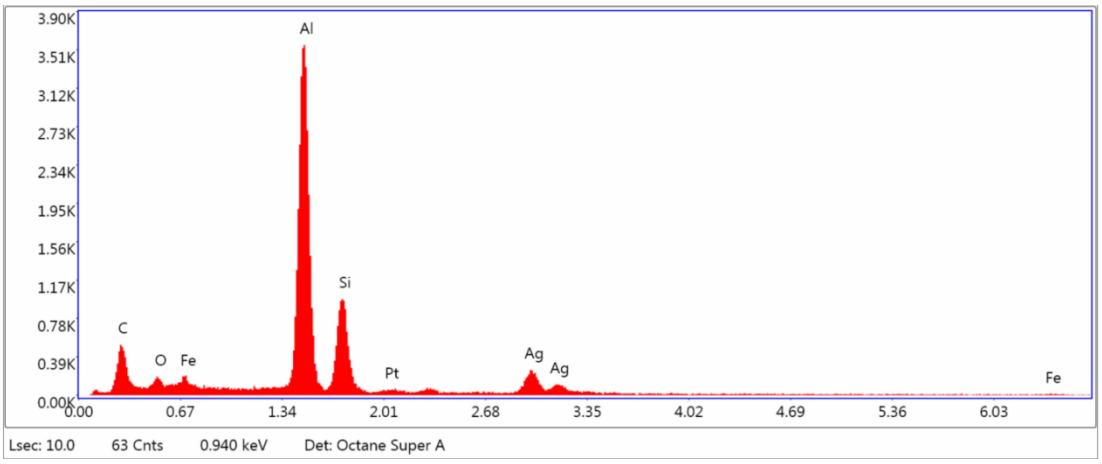

(a)

Element	Weight %	Atomic %	Net Int.	Error %	Kratio	Z	A	F
CK	21.44	40.74	272.65	12.60	0.0507	1.1880	0.1992	1.0000
OK	2.56	3.65	95.99	15.20	0.0111	1.1254	0.3855	1.0000
FeL	3.07	1.35	65.85	7.98	0.0207	0.8391	0.8054	1.0000
AlK	47.4	40.10	3218.31	3.47	0.4343	0.9840	0.9287	1.0024
SiK	14.80	12.03	792.71	6.70	0.1169	1.0029	0.7864	1.0018
PtM	0.54	0.06	8.73	43.37	0.0033	0.5930	1.0384	1.0009
AgL	10.20	2.16	141.70	14.65	0.0714	0.6993	1.0024	0.9990

(b)

Fig. 6 (a) the diagram of spectrum (b) the table of spectrum

2.3 Tensile test

This mechanical property tests were finished in Brunel University, London by a Electromechanical Universal Testing Machine of Tinius Olsen ST Series (HTE-1000). Samples were cut to a rectangle with 3cm*10cm. One piece of samples was put on the machine's fixtures with stretching critical state and stretched at a very low rate (1mm/min). With the increase of extension, the "necking" was gradually formed in the middle of sample

till it was broken (Fig 7a). Meanwhile, the data of force and extension were collected and recorded on the computer (Figure 7b).

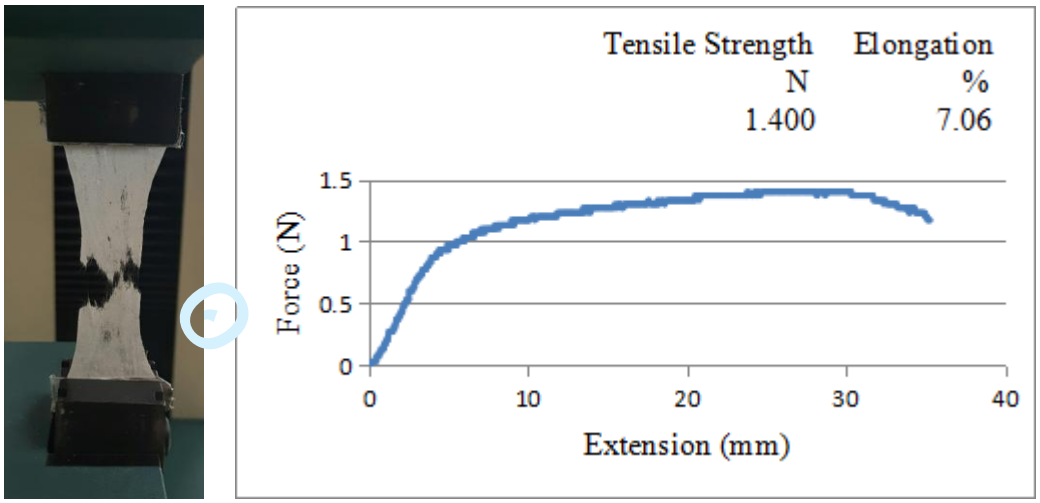

(a) (b)

Fig. 7 (a) tensile test process (b) the force-extension curve

2.4 Process of water vapour transmission test

Figure 8 shows the experimental method to test the water vapour transmission performance of the nanofibers. The same amount of distilled water was added to the same bottle whose mouths were covered with three sample groups respectively. Then the bottles were placed into an environment for 168 hours (7 days) with constant temperature (37°C) and humidity (50%) to simulate human body. Each bottle was weighed every 24 hours and its decrement can be obtained. The water vapour transmission rates, WVTRs ($g \cdot m^{-2}$ per day), were calculated as the weight loss of water (gram) per evaporation exposure area (m^2) per day.

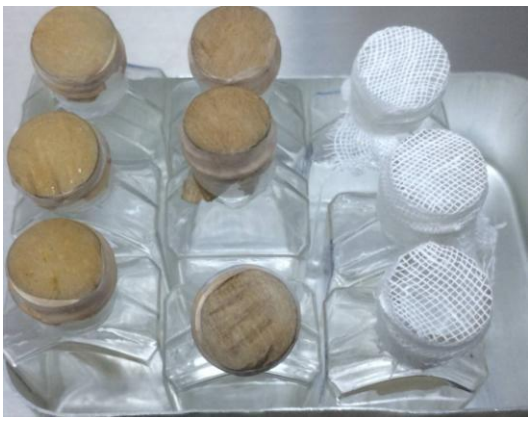

Fig. 8 water vapour transmission test

3.0 Discussions

3.1 Microstructure

The fiber diameters influence the effect of mats as simulacrum of fascia layer mainly from two aspects, the size of diameter increases the mechanical properties, the size of diameter would increase the continuous antimicrobial activity. In the condition of the same concentration of Ag, nanofibers with bigger diameters would wrap more Ag particles so that the effect of resisting bacteria is decreased resulting from the less exposed Ag particles. Therefore, to evaluate the influence factors of the diameters' size, 4 parameters were preformed to discuss the relationship between them and fiber diameters, that is, the voltage of electric field, the distance between syringe and collector, the density of EVOH solution and the concentration of Ag.

Figures 9(a)-9(c) shows the results of diameters' measurements with different densities of EVOH solution but the same other conditions. 6-10 times measuring of the fiber diameters of different parts in each picture were used for calculating trimmed mean. The findings are illustrated in Figure 9(d)-9(f). Figure 9(d) shows the influence of voltage on fiber diameter with different EVOH solution densities for the cases of the tip-to-collector distance at 25cm

and 0.02g/ml of Ag. It indicated that the most suitable voltage range is from 20~24kV. The diameters in this range are moderate than others due to the conductivity of Ag, voltage below 20kV is too low to supply enough electrostatic field force for constant stretching and collecting. If the voltage is too high, the nanofibers are easy to be broken because of the overstretched in the fabrication process. In Figure 9(e), the diameters of fibers is gradually decreased with the increase distance between syringe and collector as the voltage is 25kV and the concentration of Ag is 0.02g/ml. Comparing with 9(d), the influence of distance is less than that of voltage, especially for the samples of 12.5% EVOH solution whose trend of change is relatively gentle. Furthermore, the effect of distance for 7.5% EVOH solution is higher than the other two densities of EVOH solutions (10% and 12.5%). It seemed that the 7.5% EVOH solution is dilution so it will be stretched more easily in the spinning process. Figure 9(f) shows the influence of concentration of Ag on fiber diameter. It indicated that concentration of Ag has an obvious effect on fiber diameter to some extent. However, it is still clearly less than the influence of EVOH solution density for the fiber diameter. Besides, the EVOH solution density is also an importance influence factor through the overall analysis of the results.

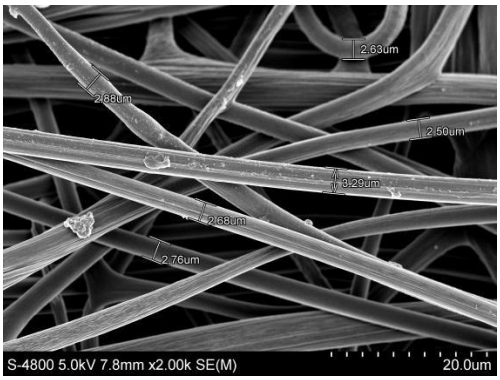

(a)

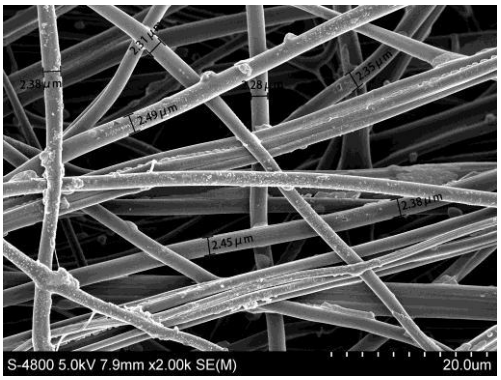

(b)

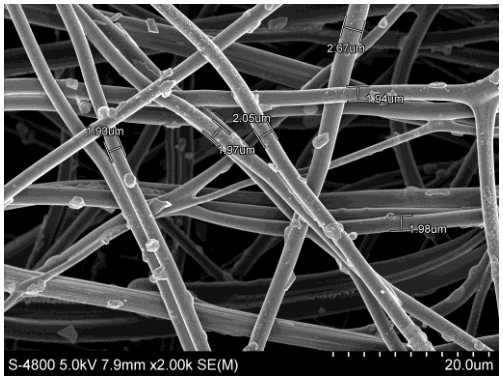

(c)

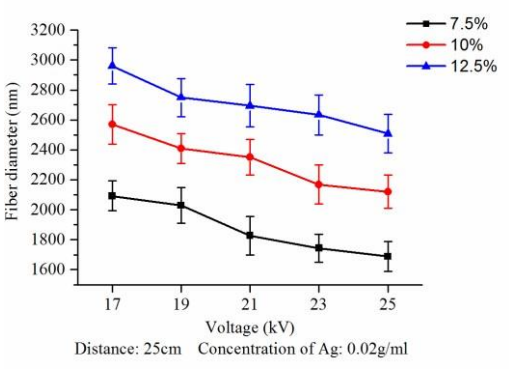

(d)

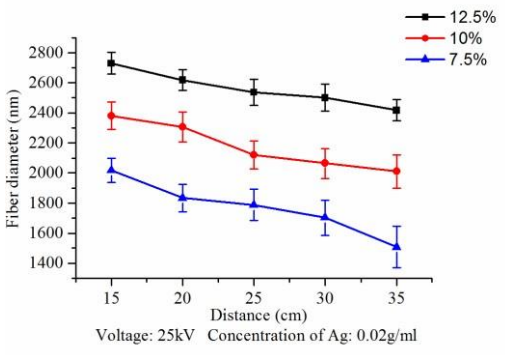

(e)

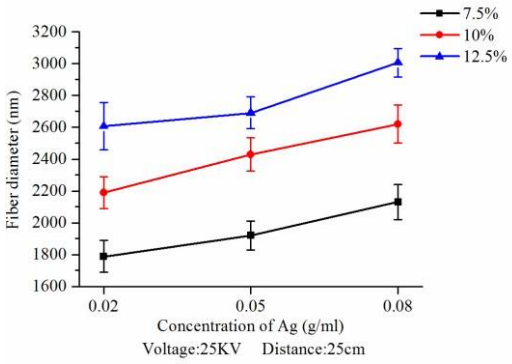

(f)

Fig. 9 (a) diameter measurement of 12.5% EVOH nanofiber mats (b) diameter measurement of 10% EVOH nanofiber mats (c) diameter measurement of 7.5% EVOH nanofiber mats (d) effect of the voltage on fiber diameters (e) effect of the distance on fiber diameters (f) effect of the concentration of Ag on fiber diameters

3.2 Tensile strength

Figure 10(a)-10(c) are the stress-strain curves of the 9 samples with different concentration of EVOH and Ag at 0.01 (1/s) strain rate. In the stress-strain curves, only the starting 20% of the deformation was considered as the true value of the elastic deformation. There are two reasons for only taking the starting 20% of deformation. First, in the dynamic stretching culture experiments that the nanofiber mats were used as the fascia layer, it only needs to work in the elastic range during the stretching process. Secondly, considering the

tensile characteristic of the fibrous materials which is approximate linear at the starting 20%, and this part is the approximate accurate value. From the observation of the three figures, it is clear that integral fracture strength of the 12.5% EVOH nanofiber mats (Figure 10a) is higher than the 7.5% and 10% EVOH nanofiber mats which fits the previous non-Ag tensile test results [22]. In Figure 10a-c, each picture illustrates the stress-strain curves with different concentration of Ag but the same density of EVOH solution. Figure 10c shows that the values of three curves of 7.5% EVOH samples which are lager difference than the 10% and 12.5% Ag EVOH nanofiber mats due to the Ag particles could provide a higher influence for a low density solution(thinner fiber diameter). Also, the Young's Moduli and yield stresses of the samples were measured by the same method with Figure 10(d). The Young's Modulus was taken as the tangent from the origin and the yield stress was obtained corresponding to 0.2% proof strain. The results of Young's Moduli and yield stresses are listed in the Table 1, it shows that with the increase of the concentration of EVOH and Ag, the Young's modulus and Yield stress were being increased in general. Combining the nanofiber diameters of each sample groups, the Young's modulus and Yield stress are affected by the fabrication parameters, such as voltage, distance between tip and collector etc. Across all the samples, EVOH content in the solutions clearly show its influence, adding Ag particle has made clear influence, the higher of the content, the higher corresponding moduli. It seems due to the silver particles exist as the "second phase" in the pure EVOH nanofiber mats. They are distributed evenly on the surface of nanofibers as the form of nanoscale particles. The silver nanoparticles are embedded in the surface of a single fiber stably. Therefore, similarly, different sizes of silver particles could connect more than two fibers at the same time, as the

circled in Figure 5. This phenomenon results in greater friction and cohesion, besides, enhances mutual containment among fibers. Thus, the tensile strength is increasing gradually with more Ag nanoparticles.

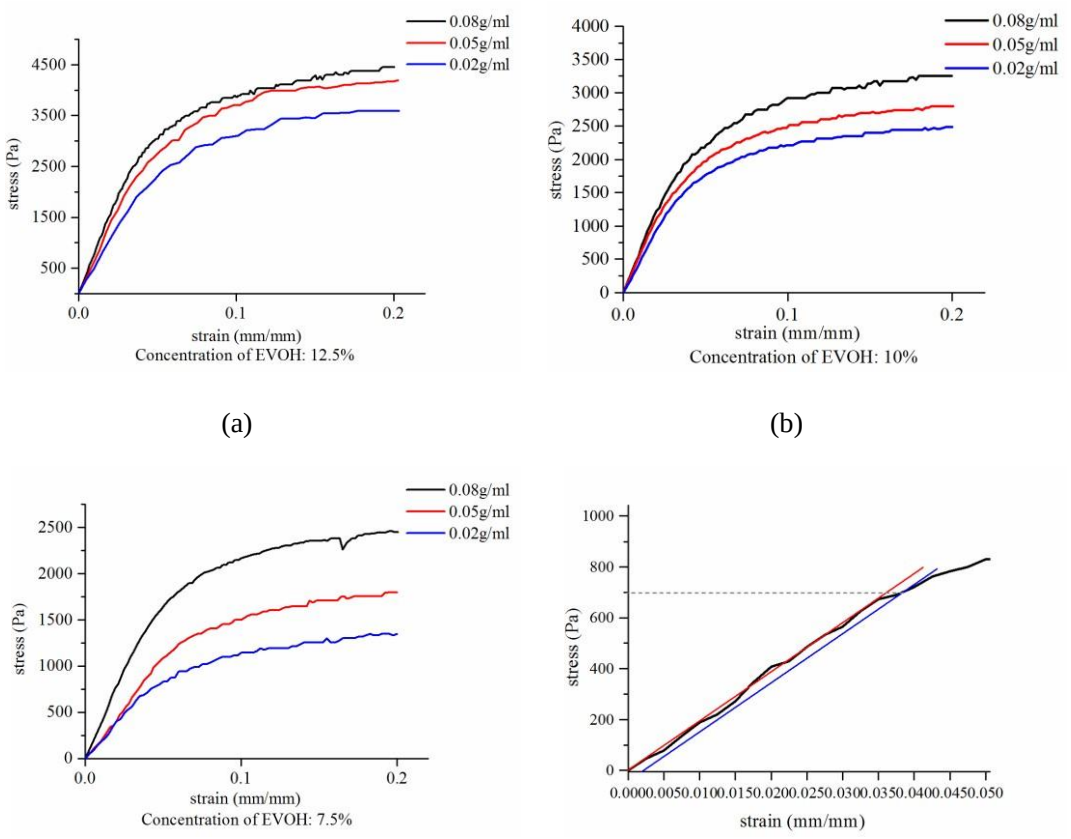

Fig. 10 (a) stress-strain of 12.5% EVOH nanofiber mats with 0.02g/ml, 0.05g/ml and 0.08g/ml of the concentration of Ag, respectively (b) stress-strain of 10% EVOH nanofiber mats with 0.02g/ml, 0.05g/ml and 0.08g/ml of the concentration of Ag, respectively (c) stress-strain of 7.5% EVOH nanofiber mats with 0.02g/ml, 0.05g/ml and 0.08g/ml of the concentration of Ag, respectively (d) Yield stress at 0.2% proof strain and moduli

Table. 1 Results of tensile test

Concentration of EVOH (%)	Concentration of Ag (g/ml)	Young's modulus (kPa)	Yield stresses (kPa)
7.5	0.02	18.631	0.699
	0.05	22.163	1.089
	0.08	38.987	1.283
10	0.02	46.189	1.372
	0.05	57.754	1.231
	0.08	64.599	1.250
12.5	0.02	57.620	1.897
	0.05	65.005	2.308
	0.08	78.300	2.319

Figure 11 shows the effect of strain rate on the moduli. With the same concentration of EVOH and Ag, the strain rate effect is weakened on the moduli, except the range of low strain rate. Comparing with different samples, we can see that the lower the concentration of EVOH and Ag, the smaller the influence of strain rate on moduli and the more gentle the curve is. Therefore, the effect of strain rate on moduli can be influenced by changing the concentration of EVOH and Ag. Moreover, the influence of EVOH concentration is even more significant than the concentration of Ag.

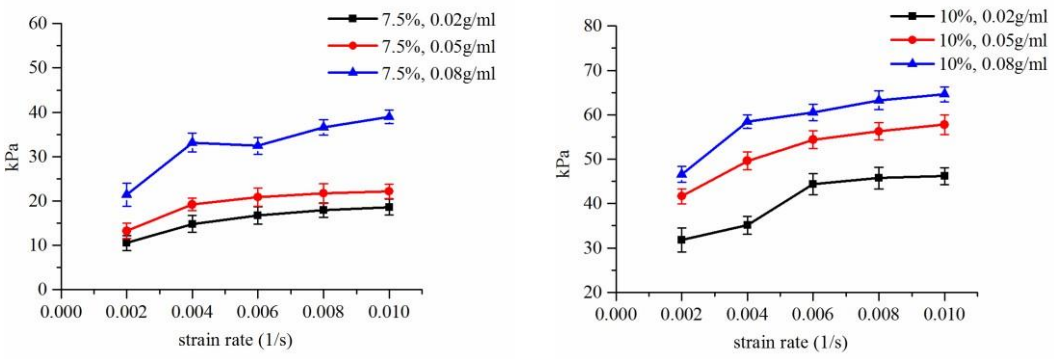

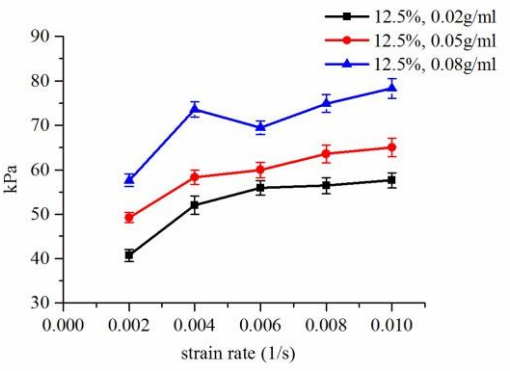

(c)

Fig. 11 moduli E vs strain rate of different samples

3.3 Water vapour transmission rates

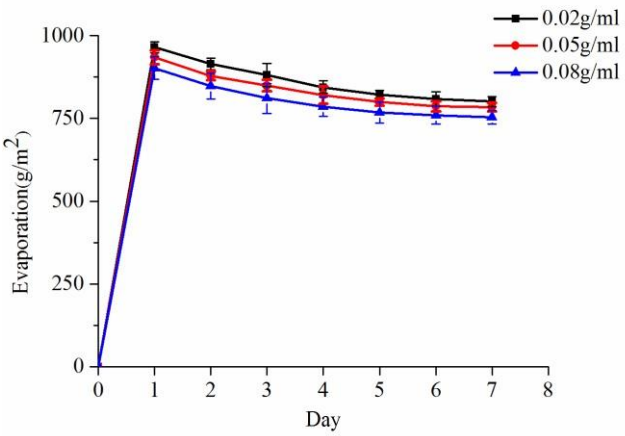

Fig. 12 Results of Water vapour transmission test with 12.5% EVOH solution density

Measured values of the water vapour transmission rates have been given in Figure 12, it shows the water vapour transmission value increased rapidly in Day 1. The 24 hour measurement span shows that there is only one data point at the end of the Day 1. Therefore, the higher points which could occur within Day 1 probably have been missed. However, the tread is captured. The water vapour transmission rate drops slightly from Day 1 and remains virtually constant from Day 2 onwards with the values kept in the range of 750 to 1000 g/m^{-2} per day. There is virtually no difference between 0.02, 0.05 and 0.08g/ml groups which is very similar to the non-Ag nanofiber mats [21], in other words, adding Ag particles may

affect other properties of the fiber mats but not the water vapour transmission rate.

4.0 Conclusions

The Ag EVOH nanofiber were obtained in the study from an electrospinning process. The experimental study carries out in the lab on the performances of mechanical properties and the water vapour transmission rates which related to the dynamic stretching culture tests, this is the foundation of the clinical applications and will have led to the following conclusions.

(1) Many factors influence the nanofiber diameter, such as voltage, tip-to-collector distance, EVOH solution density and concentration of Ag. The first three factors are positively while the concentration of Ag is negatively related to nanofiber diameter. Also, the EVOH solution density and voltage have the greatest impact.

(2) The mechanical properties of nanofiber mats were influenced by different parameters through the various diameters. So the mechanical properties can be changed greatly to match those of fascia layer of human body to simulate better.

(3) The effect of strain rate on moduli is weak for one sample except at low range (0.02-0.04 1/s). Also, for different samples, with the decreased concentration of EVOH and Ag, the effect of strain rate on moduli will be smaller.

(4) The water vapour transmission rates of nanofiber mats are comparable and equally similar to the non-Ag EVOH nanofiber mats.

In a word, the mechanical properties of nanofiber mats encapsulated Ag particles can achieve the standard that used for simulating fascia layer. Moreover, according to different requirements for different parts of human body, the properties could be adjusted by changing

fabrication parameters. In the next stage of our work, we will be focusing on the cell growth on the fiber mats and cell alignment on the parallel nanofiber mats.

Acknowledgement

This research was supported by the The Natural Science Project of Education Office of Shaanxi Province under Grant No.15JK1484.

References

1. Tournadre A., J.J. Dubost, and M. Soubrier, 'Treatment of inflammatory muscle disease in adults', *Joint Bone Spine*, 2010, 77(5): p. 390-4.
2. Barone A.L. et al., 'The gracilis myocutaneous free flap in swine: an advantageous preclinical model for vascularized composite allograft transplantation research', *Microsurgery*, 2013, 33(1): p. 51-55.
3. Wang, Y. et al., 'A biomimetic silk fibroin/sodium alginate composite scaffold for soft tissue engineering', *Sci Rep*, 2016, 6: p. 39477.
4. Shah, G., B.J. Costello, 'Soft tissue regeneration incorporating 3-dimensional biomimetic scaffolds', *Oral Maxillofac Surg Clin North Am*, 2017, 29(1): p. 9-18.
5. Wang, L. et al., 'Nanofiber yarn/hydrogel core-shell scaffolds mimicking native skeletal muscle tissue for guiding 3D myoblast alignment, elongation and differentiation', *ACS Nano*, 2015, 9(9): p. 9167-79.
6. Claudia Fuoco, Lucia Lisa Petrilli and Stefano Cannata, 'Matrix scaffolding for stem cell guidance toward skeletal muscle tissue engineering', *Journal of Orthopaedic Surgery and Research*, 2016, 11(1).
7. Wang, P.Y., H.T. Yu and W.B. Tsai, 'Modulation of alignment and differentiation of skeletal myoblasts by submicron ridges/grooves surface structure', *Biotechnol Bioeng*, 2010, 106(2): p. 285-94.
8. Shen, J.Y. et al., 'UV-embossed microchannel in biocompatible polymeric film: application to control of cell shape and orientation of muscle cells', *J Biomed Mater Res B Appl Biomater*, 2006, 77(2): p. 423-30.
9. Aviss, K.J., J.E. Gough and S. Downes, 'Aligned electrospun polymer fibres for skeletal muscle regeneration', *Eur Cell Mater*, 2010, 19: p. 193-204.
10. Aaron S. Goldstein, Patrick S. Thayer, 'Chapter 11: Fabrication of complex biomaterial scaffold for soft tissue engineering by electrospinning', *Nanobiomaterials in Soft Tissue Engineering*, 2016: 299-330.
11. Ran Huang, Xiaomin Zhu and Haiyan Tu, 'The crystallization behaviour of porous poly(lactic acid) prepared by modified solvent casting/particulate leaching technique for potential use of tissue engineering scaffold', *Materials Letters*, 2014, 136(1): 126-129.
12. Altomare, L. et al., 'Biodegradable microgrooved polymeric surfaces obtained by photolithography for skeletal muscle cell orientation and myotube development', *Acta Biomater*, 2010, 6(6): p. 1948-57.

13. Cristina Borselli, Christine A. Cezar and Dymitri Shvartsman, 'The role of multifunctional delivery scaffold in the ability of cultured myoblasts to promote muscle regeneration', *Biomaterials*, 2011, 32(34): 8905-8914.
14. Woojin M. Han, Young C. Jang and Andres J. Garcia, 'Engineered matrices for skeletal muscle satellite cell engraftment and function', *Matrix Biology*, 2017, 60-61: 96-109.
15. Pennisi C.P. et al., 'Uniaxial cyclic strain drives assembly and differentiation of skeletal myocytes', *Tissue Eng Part A*, 2011, 17(19-20): p. 2543-50.
16. Morioka, M. et al., 'Microtubule dynamics regulate cyclic stretch-induced cell alignment in human airway smooth muscle cells', *PLoS One*, 2011, 6(10): p. e26384.
17. Ahadian, S. et al., 'Interdigitated array of Pt electrodes for electrical stimulation and engineering of aligned muscle tissue', *Lab Chip*, 2012. 12(18): p. 3491-503.
18. Ramon-Azcon et al., 'Gelatin methacrylate as a promising hydrogel for 3D microscale organization and proliferation of dielectrophoretically patterned cells', *Lab Chip*, 2012, 12(16): p. 2959-69.
19. Mueller, Cornelia Emika and Birk Richard, 'Influence of static magnetic fields on human myoblast/mesenchymal stem cell co-cultures', *Molecular Medicine Reports*, 2018, 17: 3813-3820.
20. Dong, G., Lian, Q. and Yang L, 'Design and fabrication of vascular network for muscle tissue engineering', Proceedings of the 2016 International Forum on Energy Environment and Sustainable Development, *Series in AER-Advances in Engineering Research*, 75 (2016) 613-621.
21. Anhui Wang, Chao Xu and Chuanwei Zhang, 'Experimental investigation of the properties of electrospun nanofibers for potential medical application', *Journal of Nanomaterials*, 2015, 10: 1155-1163.
22. B. Wang, X. Chao and Y. Li, 'Tensile strength of electrospun poly(ethylene-co-vinyl alcohol) nanofibre sheets', *Key Engineering Materials*, 2013, 10: 535-536.
23. Chao Xu, Feng Xu and Bin Wang, 'Electrospinning of poly(ethylene-co-vinyl alcohol) nanofibres encapsulated with Ag nanoparticles for skin wound healing', *Journal of Nanomaterials*, 2011, 10: 1155-1162.
24. Tan Lin, Hu Jinlian and Zhao Huafu, 'Design of bilayered nanofibrous mats for wound dressing using an electrospinning technique', *Material letters*, 2015, 156: 46-49.
25. Tao Jiang, Erica J. Carbone, Kevin W.-H. Lo, Cato T. Laurencin, 'Electrospinning of polymer nanofibers for tissue regeneration', *Progress in Polymer Science*, 2015, 46: 1-24.
26. Lixin Xia, Meng Xu and Guangzhen Cheng, 'Facile construction of Ag nanoparticles encapsulated into carbon nanotubes with robust antibacterial activity', *Carbon*, 2018, 130: 775-781.